

Axisymmetric steady temperature field in FGM cylindrical shells with temperature-dependent heat conductivity and arbitrary linear boundary conditions

A. MOOSAIE

*Department of Mechanical Engineering
Yasouj University
75914-353 Yasouj, Iran
e-mail: moosaie@yu.ac.ir*

AN APPROXIMATE ANALYTICAL SOLUTION to the axisymmetric heat conduction equation for a hollow cylinder made of functionally graded material with temperature-dependent heat conductivity is presented. General linear boundary conditions are considered. The Poincaré method for regular perturbation problems is employed to obtain an analytical closed-form approximate solution for the temperature field. The hierarchical asymptotic problems are solved up to the second-order approximation. A numerical example is worked out, i.e., the one-dimensional heat conduction in the radial direction with prescribed temperatures at the boundaries. The approximate temperature profiles are compared with a numerical solution of the full nonlinear problem which provides the reference “exact” solution. A good agreement between the approximate and reference solutions is established. The convergence of the asymptotic series as well as the properties of the temperature field are studied.

Key words: heat conduction, temperature-dependent heat conductivity, functionally graded material, hollow cylinder, perturbation method.

Copyright © 2015 by IPPT PAN

1. Introduction

THERE ARE CERTAIN CIRCUMSTANCES in the modern engineering practice where a simple homogeneous material such as steel cannot fulfill all the technical requirements imposed by constantly growing applications. This limitation can be to some extent alleviated by using anisotropic laminated or fiber-reinforced composites in engineering designs. Despite their usefulness in a large variety of applications, these composites have their own limitations and shortcomings. For example, they are prone to stress concentration due to material discontinuities and delamination. A novel remedy against these problems is to use a class of advanced composites called functionally graded materials (FGMs). These materials are usually isotropic, but always inhomogeneous. That is, the material properties vary continuously in space so that certain objectives can be achieved in the design process. For example, the inner surface of a pressure vessel or

a pipe can be made of ceramics whereas the outer surface is made of a metal like steel. Such a design can withstand extreme conditions to which the inner surface is exposed like high temperatures or hazardous environment while the outer steel guarantees the structural integrity of the vessel. Moreover, the outer surface made of steel can be bolted or welded in order to provide appropriate mechanical constraints to the foundations whatsoever. Such a material leaves a lot of options and flexibilities at our disposal. For a functionally graded material however, the blending between ceramics and metal has to vary continuously and smoothly in space.

An important feature of FGMs is to resist high temperatures and the so-induced thermal stresses. Thus, thermal and eventually thermoelastic analysis of structures made of FGMs are of paramount importance. The first step in such an analysis is to solve the heat conduction problem within the material so as to determine the temperature field. Once the temperature field is known, the analysis can be extended further to calculate the thermal stresses, strains and displacements. This information is needed in order to design a pressure vessel or any other structure intended to carry thermal extreme loads.

It is obvious that in real-world engineering problems, we work with real-world materials. Therefore, many idealizations, assumptions and simplifications that are employed in the daily practice of mechanics might not be feasible anymore. By the advancement of technology and the increasing need for more reliable and economic designs with possibly small safety factors, the accuracy of thermal and mechanical analyses is highly demanded. For example, the classical assumption of temperature-independent material properties that is often made in engineering calculations becomes problematic, especially when the structure undergoes large temperature differences. So, if a more accurate calculation is the aim, the temperature-dependency of material properties is to be taken into account. In this paper, the steady axisymmetric heat conduction problem within an infinitely long cylindrical shell made of FGM with temperature-dependent material properties is studied by analytical means. For this purpose, the Poincaré method is used for regular perturbation problems. This solution is interesting from the viewpoint of heat transfer analysis of pressure vessels and it is also useful to pave the way toward analytical solution of thermal stresses within the FGM cylinder with temperature-dependent material properties.

The axisymmetric temperature field due to heat conduction in the radial direction of a homogeneous cylindrical shell has been studied for a long time and is now merely considered as a textbook material. However, the analytical determination of the temperature field and subsequently the induced thermal stresses in cylindrical objects made of functionally graded materials is a matter of contemporary research works. Virtually all papers published in this field address the case with temperature-independent material properties. Though, a number of

numerical studies have been conducted to investigate the effect of temperature on the material properties, cf. [1]. In what follows, a brief review of relevant analytical works is presented.

Using perturbation technique, OBATA and NODA [2] analyzed steady one-dimensional thermal stresses in hollow cylindrical and spherical objects. OOTAO *et al.* [3] made a transient analysis of thermal stresses in a functionally graded hollow cylinder due to a moving heat source in the axial direction. LUTZ and ZIMMERMANN [4, 5] gave the analytical solution for the thermal stresses in thick cylindrical and spherical shells made of FGMs graded in the radial direction. TANIGAWA *et al.* [6] analytically investigated thermal stresses in a FGM semi-infinite body graded with a power function in the thickness direction. JABBARI *et al.* [7, 8] considered an FGM hollow cylinder graded by a power function in the radial direction and developed analytical solutions for one- and two-dimensional thermal stresses. LIEW *et al.* [9] presented an analysis of thermoelastic problem in an FGM hollow cylinder. They proposed a novel technique by which they derived the solution for an inhomogeneous material from the solution for a homogeneous material. YOU *et al.* [10] gave an analytical solution for elastic stresses in thick-walled spherical vessels under internal pressure. They considered the shell to be made of a functionally graded material confined between two inner and outer homogeneous layers. ZHAO *et al.* [11] have analytically studied the transient temperature field in objects of different shapes made of FGM under convective boundary conditions. CHEN and LIN [12] performed an elastic analysis of a thick-walled FGM cylindrical shell graded exponentially in the radial direction. ASGARI and AKHLAGHI [13] have analytically studied transient heat conduction in a two-dimensional FGM hollow cylinder with finite length. PENG and LI [14] proposed a method to solve steady thermal stresses in a hollow cylinder made of functionally graded materials with physical properties varying in the radial direction.

The remainder of this paper is organized as follows. The governing equations are presented in Section 2. The analytical solution is given in Section 3. Section 5 contains a numerical example which is worked out using the proposed solution procedure. Finally, the paper is concluded in Section 6.

2. Governing equations

In this section, the differential equation governing the heat conduction problem in a hollow cylinder made of FGM with temperature-dependent material properties along with the required boundary conditions are presented. This equation is to be solved in order to obtain the temperature field within the hollow cylinder. The inner and outer radii of the cylinder are respectively denoted by R_i and R_o throughout this paper.

When a steady heat conduction analysis is the aim, the only relevant material property is the heat conductivity λ . First, we shall introduce the FGM model which is used to describe the spatial variation of the heat conductivity within the cylinder. Also, the dependence of λ on temperature is to be pointed out.

For a cylinder which is functionally graded in the radial direction r and whose heat conductivity depends upon temperature, the heat conductivity λ can be written as $\lambda = \lambda(\vartheta, r)$, with ϑ being the temperature field. Furthermore, if the material property function is separable, λ can then be shown as

$$(2.1) \quad \lambda = \lambda(\vartheta, r) = f(\vartheta)g(r),$$

in which $f(\vartheta)$ delegates the dependency of λ upon the temperature and $g(r)$ is the grading function. The following model for temperature-dependent, functionally graded heat conductivity is employed throughout this paper:

$$(2.2) \quad \lambda = \lambda(\vartheta, r) = (\lambda_0 - \lambda_1\vartheta) \left(\frac{r}{R_o} \right)^m,$$

where λ_0 , λ_1 and m are physical constants characterizing the material behavior. Equation (2.2) describes a material in which the heat conductivity depends on temperature in a linear manner, that is, λ decreases by increasing temperature if $\lambda_1 > 0$ and vice versa. The case with $\lambda_1 = 0$ simply describes a material with temperature-independent heat conductivity. The power m determines how the heat conductivity changes with radius r . In the grading function g , the radius r is non-dimensionalized by the outer radius R_o . Normally, λ_1 is very small compared to λ_0 , i.e., $\lambda_1 \ll \lambda_0$. This means that the heat conductivity is basically $\lambda_0 g(r)$ at a reference temperature and it is perturbed by the term $-\lambda_1 \vartheta g(r)$ when the temperature changes from the reference value by an amount of ϑ .

The differential equation governing the temperature field is obtained by the energy conservation law, the Fourier constitutive equation for heat conduction and the dependence of heat conductivity on spatial coordinates and temperature as pointed out in equation (2.2). Thus, we start with the steady energy conservation law without heat generation:

$$(2.3) \quad \nabla \cdot \mathbf{q} = 0,$$

where ∇ and \mathbf{q} are the nabla operator and heat flux vector, respectively. Equation (2.3) shows that for steady heat conduction without heat generation, the heat flux vector \mathbf{q} is a solenoidal or divergence-free vector field.

Equation (2.3) is a single scalar equation for three components of the heat flux vector \mathbf{q} . Thus, equation (2.3) is unclosed and in order to mathematically close this system, a constitutive equation relating the heat flux vector to the

temperature is required. In this work, the classical Fourier heat conduction law is used:

$$(2.4) \quad \mathbf{q} = -\boldsymbol{\lambda} \cdot \nabla \vartheta,$$

in which $\boldsymbol{\lambda}$ is the heat conductivity tensor. For isotropic materials, the heat conductivity tensor $\boldsymbol{\lambda}$ reduces to a spherical tensor, i.e.

$$(2.5) \quad \boldsymbol{\lambda} = \lambda \mathbf{E},$$

with λ and \mathbf{E} being the heat conductivity of the isotropic material and the identity tensor, respectively. Substituting equation (2.5) into equation (2.4) yields

$$(2.6) \quad \mathbf{q} = -\lambda \mathbf{E} \cdot \nabla \vartheta = -\lambda \nabla \vartheta.$$

The Fourier constitutive equation (2.6) along with the energy conservation law (2.3) gives the following field equation for the temperature:

$$(2.7) \quad \nabla \cdot (\lambda \nabla \vartheta) = 0.$$

For an infinitely long cylinder with axisymmetric temperature field, equation (2.7) reduces to the following nonlinear ordinary differential equation:

$$(2.8) \quad \frac{1}{r} \frac{d}{dr} \left(r \lambda(\vartheta, r) \frac{d\vartheta}{dr} \right) = 0.$$

Differentiating $(r \lambda d\vartheta/dr)$ with respect to r using the product rule, equation (2.8) can be written as

$$(2.9) \quad \frac{d}{dr} \left(r \lambda \frac{d\vartheta}{dr} \right) = \lambda \frac{d\vartheta}{dr} + r \frac{d\lambda}{dr} \frac{d\vartheta}{dr} + r \lambda \frac{d^2\vartheta}{dr^2} = 0,$$

in which $d\lambda/dr$ is calculated using the product rule:

$$(2.10) \quad \begin{aligned} \frac{d\lambda}{dr} &= \frac{d}{dr} \left[(\lambda_0 - \lambda_1 \vartheta) \left(\frac{r}{R_o} \right)^m \right] \\ &= \frac{d(\lambda_0 - \lambda_1 \vartheta)}{dr} \left(\frac{r}{R_o} \right)^m + (\lambda_0 - \lambda_1 \vartheta) \frac{d}{dr} \left(\frac{r}{R_o} \right)^m. \end{aligned}$$

Furthermore, the use of the chain rule of differentiation yields

$$(2.11) \quad \frac{d(\lambda_0 - \lambda_1 \vartheta)}{dr} = \frac{d(\lambda_0 - \lambda_1 \vartheta)}{d\vartheta} \frac{d\vartheta}{dr} = -\lambda_1 \frac{d\vartheta}{dr}.$$

Substituting equations (2.10) and (2.11) into equation (2.9) gives

$$(2.12) \quad \left[(1 + m)(\lambda_0 - \lambda_1 \vartheta) - r \lambda_1 \frac{d\vartheta}{dr} \right] \frac{d\vartheta}{dr} + r(\lambda_0 - \lambda_1 \vartheta) \frac{d^2\vartheta}{dr^2} = 0.$$

Equation (2.12) shows that taking into account the temperature-dependency of the heat conductivity results in governing equation becoming nonlinear. Thus, the analysis of the problem gets much more difficult than the case with temperature-independent heat conductivity. Due to this inherent difficulty, it is often tried to refrain from such a full nonlinear description. However, the advancement of technology pushes us toward a more accurate description for the behavior of engineering materials.

In order to be solved, equation (2.12) requires two boundary conditions in r direction. In this paper, we consider general linear boundary conditions imposed on inner and outer surfaces of the cylinder:

$$(2.13a) \quad \alpha_i \vartheta(r = R_i) + \beta_i \left. \frac{d\vartheta}{dr} \right|_{r=R_i} = \gamma_i,$$

$$(2.13b) \quad \alpha_o \vartheta(r = R_o) + \beta_o \left. \frac{d\vartheta}{dr} \right|_{r=R_o} = \gamma_o,$$

where α_i , α_o , β_i , β_o , γ_i and γ_o are some constant coefficients. These general boundary conditions cover the cases with prescribed temperature, prescribed heat flux and heat convection at the boundaries by choosing appropriate values for the coefficients. For example, by choosing $\alpha_i = 1$, $\beta_i = 0$, $\alpha_o = 0$ and $\beta_o = 1$, we have a prescribed temperature at the inner surface whereas the heat flux is specified at the outer surface.

3. Analytical solution using perturbation technique

In this section, the heat conduction problem is going to be solved in order to obtain the temperature field ϑ . The heat conduction problem is solved using the Poincaré method for regular perturbation problems. For this purpose, a small parameter ε is to appear in the nonlinear differential equation (2.8). As mentioned earlier, one can postulate that $\lambda_1 \ll \lambda_0$ for most of engineering materials. The rationale for this assumption is as follows. The heat conductivity at a reference temperature ϑ_0 is $\lambda_0 g(r)$ and by varying the temperature, it changes to a new function $(\lambda_0 - \lambda_1 \vartheta)g(r)$. However, as long as the temperature variation from the reference value is not very intense, one expects that the change in heat conductivity is small. Thus, λ_1 has to be small compared to λ_0 . We can now define the small parameter ε as

$$(3.1) \quad \varepsilon = \frac{\lambda_1}{\lambda_0} \ll 1.$$

Dividing both sides of equation (2.12) by the non-zero constant λ_0 , we can obtain the governing equation of the temperature field in terms of the small

parameter ε :

$$(3.2) \quad \left[(1+m)(1-\varepsilon\vartheta) - \varepsilon r \frac{d\vartheta}{dr} \right] \frac{d\vartheta}{dr} + r(1-\varepsilon\vartheta) \frac{d^2\vartheta}{dr^2} = 0.$$

Equation (3.2) is a nonlinear ordinary differential equation and the regular perturbation method (Poincaré’s technique) is employed to solve it. For this purpose, the temperature field ϑ is expanded as a power series of ε :

$$(3.3) \quad \vartheta = \bar{\vartheta}_0 + \varepsilon\bar{\vartheta}_1 + \varepsilon^2\bar{\vartheta}_2 + \dots = \sum_{n=0}^{\infty} \varepsilon^n \bar{\vartheta}_n.$$

This expansion can be truncated at any order to give an approximate temperature field, e.g.:

$$(3.4) \quad \vartheta_0 = \bar{\vartheta}_0,$$

$$(3.5) \quad \vartheta_1 = \bar{\vartheta}_0 + \varepsilon\bar{\vartheta}_1,$$

$$(3.6) \quad \vartheta_2 = \bar{\vartheta}_0 + \varepsilon\bar{\vartheta}_1 + \varepsilon^2\bar{\vartheta}_2.$$

Substituting expansion (3.3) into equation (3.2) and grouping all terms with the same power of ε gives

$$(3.7) \quad \begin{aligned} & \varepsilon^0 \left[r \frac{d^2\bar{\vartheta}_0}{dr^2} + (1+m) \frac{d\bar{\vartheta}_0}{dr} \right] \\ & + \varepsilon^1 \left[r \frac{d^2\bar{\vartheta}_1}{dr^2} + (1+m) \frac{d\bar{\vartheta}_1}{dr} - \bar{\vartheta}_0 \left(r \frac{d^2\bar{\vartheta}_0}{dr^2} + (1+m) \frac{d\bar{\vartheta}_0}{dr} \right) - r \frac{d\bar{\vartheta}_0}{dr} \frac{d\bar{\vartheta}_0}{dr} \right] \\ & + \varepsilon^2 \left[r \frac{d^2\bar{\vartheta}_2}{dr^2} + (1+m) \frac{d\bar{\vartheta}_2}{dr} - \bar{\vartheta}_0 \left(r \frac{d^2\bar{\vartheta}_1}{dr^2} + (1+m) \frac{d\bar{\vartheta}_1}{dr} \right) \right. \\ & \quad \left. - \bar{\vartheta}_1 \left(r \frac{d^2\bar{\vartheta}_0}{dr^2} + (1+m) \frac{d\bar{\vartheta}_0}{dr} \right) - 2r \frac{d\bar{\vartheta}_0}{dr} \frac{d\bar{\vartheta}_1}{dr} \right] + O(\varepsilon^3) = 0. \end{aligned}$$

This series can be continued and more terms could be obtained. In this paper, we restrict ourselves to the above order of approximation and do not go any further.

Since equation (3.7) is to hold for arbitrary values of ε , each square-bracketed term is to vanish individually. This results in a hierarchical series of problems which we solve in the sequel in order to obtain different levels of approximation for the temperature field. First, the $O(\varepsilon^0)$ problem is to be solved:

$$(3.8) \quad O(\varepsilon^0) : \quad r \frac{d^2\bar{\vartheta}_0}{dr^2} + (1+m) \frac{d\bar{\vartheta}_0}{dr} = 0,$$

which can also be obtained by setting $\varepsilon = 0$ in equation (3.7). This is a homogeneous Cauchy–Euler ordinary differential equation whose general solution reads

$$(3.9) \quad \bar{\vartheta}_0(r) = C_{1,0} + \frac{C_{2,0}}{r^m}.$$

To determine the integration constants $C_{1,0}$ and $C_{2,0}$, this general solution must be subjected to the following boundary conditions:

$$(3.10a) \quad \alpha_i \bar{\vartheta}_0(r = R_i) + \beta_i \left. \frac{d\bar{\vartheta}_0}{dr} \right|_{r=R_i} = \gamma_i,$$

$$(3.10b) \quad \alpha_o \bar{\vartheta}_0(r = R_o) + \beta_o \left. \frac{d\bar{\vartheta}_0}{dr} \right|_{r=R_o} = \gamma_o.$$

Imposition of these boundary conditions onto the general solution (3.9) gives the following relations for the integration constants $C_{1,0}$ and $C_{2,0}$:

$$(3.11) \quad C_{1,0} = \frac{\zeta_o \gamma_i - \zeta_i \gamma_o}{\alpha_i \zeta_o - \alpha_o \zeta_i}, \quad C_{2,0} = \frac{\alpha_i \gamma_o - \alpha_o \gamma_i}{\alpha_i \zeta_o - \alpha_o \zeta_i},$$

in which

$$(3.12) \quad \zeta_i = \frac{\alpha_i R_i - \beta_i m}{R_i^{m+1}}, \quad \zeta_o = \frac{\alpha_o R_o - \beta_o m}{R_o^{m+1}}.$$

The $O(\varepsilon^1)$ problem is obtained by setting the bracket multiplied by ε^1 in equation (3.7) to zero:

$$(3.13) \quad O(\varepsilon^1) : r \frac{d^2 \bar{\vartheta}_1}{dr^2} + (1+m) \frac{d\bar{\vartheta}_1}{dr} = \bar{\vartheta}_0 \left(r \frac{d^2 \bar{\vartheta}_0}{dr^2} + (1+m) \frac{d\bar{\vartheta}_0}{dr} \right) + r \frac{d\bar{\vartheta}_0}{dr} \frac{d\bar{\vartheta}_0}{dr}.$$

The first term on the right-hand side of equation (3.13) vanishes due to equation (3.8). Thus, the $O(\varepsilon^1)$ problem can be finally written as

$$(3.14) \quad O(\varepsilon^1) : r \frac{d^2 \bar{\vartheta}_1}{dr^2} + (1+m) \frac{d\bar{\vartheta}_1}{dr} = r \frac{d\bar{\vartheta}_0}{dr} \frac{d\bar{\vartheta}_0}{dr},$$

which is an inhomogeneous Cauchy-Euler differential equation whose solution is composed of two parts: the homogeneous solution and a particular solution. The homogeneous solution of equation (3.14) is the same as the solution of equation (3.8). A particular solution of equation (3.13) can be easily calculated as well. The general solution of equation (3.13) then reads

$$(3.15) \quad \bar{\vartheta}_1(r) = C_{1,1} + \frac{C_{2,1}}{r^m} + \frac{C_{2,0}^2}{2r^{2m}},$$

which is to be subjected to the following boundary conditions:

$$(3.16a) \quad \alpha_i \bar{\vartheta}_1(r = R_i) + \beta_i \left. \frac{d\bar{\vartheta}_1}{dr} \right|_{r=R_i} = 0,$$

$$(3.16b) \quad \alpha_o \bar{\vartheta}_1(r = R_o) + \beta_o \left. \frac{d\bar{\vartheta}_1}{dr} \right|_{r=R_o} = 0.$$

Application of these boundary conditions to the general solution (3.15) yields the following relations for the integration constants:

$$(3.17) \quad C_{1,1} = \frac{\zeta_o \xi_i - \zeta_i \xi_o}{\alpha_i \zeta_o - \alpha_o \zeta_i}, \quad C_{2,1} = \frac{\alpha_i \xi_o - \alpha_o \xi_i}{\alpha_i \zeta_o - \alpha_o \zeta_i},$$

where

$$(3.18) \quad \xi_i = \frac{(2\beta_i m - \alpha_i R_i) C_{2,0}^2}{2R_i^{2m+1}}, \quad \xi_o = \frac{(2\beta_o m - \alpha_o R_o) C_{2,0}^2}{2R_o^{2m+1}}.$$

Finally, we look at the $O(\varepsilon^2)$ problem. In order to obtain the $O(\varepsilon^2)$ problem we need to set the terms multiplied by ε^2 in equation (3.7) to zero. This gives

$$(3.19) \quad O(\varepsilon^2) : \quad r \frac{d^2 \bar{\vartheta}_2}{dr^2} + (1+m) \frac{d\bar{\vartheta}_2}{dr} = \bar{\vartheta}_0 \left(r \frac{d^2 \bar{\vartheta}_1}{dr^2} + (1+m) \frac{d\bar{\vartheta}_1}{dr} \right) \\ + \bar{\vartheta}_1 \left(r \frac{d^2 \bar{\vartheta}_0}{dr^2} + (1+m) \frac{d\bar{\vartheta}_0}{dr} \right) + 2r \frac{d\bar{\vartheta}_0}{dr} \frac{d\bar{\vartheta}_1}{dr}.$$

This equation can be rewritten in the following form by taking into account equations (3.8) and (3.14):

$$(3.20) \quad O(\varepsilon^2) : \quad r \frac{d^2 \bar{\vartheta}_2}{dr^2} + (1+m) \frac{d\bar{\vartheta}_2}{dr} = r \bar{\vartheta}_0 \frac{d\bar{\vartheta}_0}{dr} \frac{d\bar{\vartheta}_0}{dr} + 2r \frac{d\bar{\vartheta}_0}{dr} \frac{d\bar{\vartheta}_1}{dr} \\ = r \frac{d\bar{\vartheta}_0}{dr} \left(\bar{\vartheta}_0 \frac{d\bar{\vartheta}_0}{dr} + 2 \frac{d\bar{\vartheta}_1}{dr} \right).$$

This is again an inhomogeneous Cauchy-Euler differential equation whose general solution is written as the sum of the homogeneous solution and a particular solution:

$$(3.21) \quad \bar{\vartheta}_2(r) = C_{1,2} + \frac{C_{2,2}}{r^m} + \frac{\chi}{2r^{2m}} + \frac{C_{2,0}^3}{2r^{3m}},$$

in which

$$(3.22) \quad \chi = C_{2,0}(C_{1,0}C_{2,0} + 2C_{2,1}).$$

The boundary conditions for the $O(\varepsilon^2)$ problem are

$$(3.23a) \quad \alpha_i \bar{\vartheta}_2(r = R_i) + \beta_i \left. \frac{d\bar{\vartheta}_2}{dr} \right|_{r=R_i} = 0,$$

$$(3.23b) \quad \alpha_o \bar{\vartheta}_2(r = R_o) + \beta_o \left. \frac{d\bar{\vartheta}_2}{dr} \right|_{r=R_o} = 0,$$

which give the following values for the integration constants $C_{1,2}$ and $C_{2,2}$:

$$(3.24) \quad C_{1,2} = \frac{\zeta_o \eta_i - \zeta_i \eta_o}{\alpha_i \zeta_o - \alpha_o \zeta_i}, \quad C_{2,2} = \frac{\alpha_i \eta_o - \alpha_o \eta_i}{\alpha_i \zeta_o - \alpha_o \zeta_i},$$

where

$$(3.25) \quad \eta_i = \frac{(2\beta_i m - \alpha_i R_i) \chi}{2R_i^{2m+1}} + \frac{(3\beta_i m - \alpha_i R_i) C_{2,0}^3}{2R_i^{3m+1}},$$

$$\eta_o = \frac{(2\beta_o m - \alpha_o R_o) \chi}{2R_o^{2m+1}} + \frac{(3\beta_o m - \alpha_o R_o) C_{2,0}^3}{2R_o^{3m+1}}.$$

Now, the temperature fields at different orders of approximation read

$$(3.26) \quad \vartheta_0(r) = \varepsilon^0 \bar{\vartheta}_0 = \varepsilon^0 \left(C_{1,0} + \frac{C_{2,0}}{r^m} \right) + O(\varepsilon^1),$$

$$(3.27) \quad \vartheta_1(r) = \bar{\vartheta}_0 + \varepsilon^1 \bar{\vartheta}_1$$

$$(3.28) \quad = \varepsilon^0 \left(C_{1,0} + \frac{C_{2,0}}{r^m} \right) + \varepsilon^1 \left(C_{1,1} + \frac{C_{2,1}}{r^m} + \frac{C_{2,0}^2}{2r^{2m}} \right) + O(\varepsilon^2),$$

$$(3.29) \quad \vartheta_2(r) = \bar{\vartheta}_0 + \varepsilon^1 \bar{\vartheta}_1 + \varepsilon^2 \bar{\vartheta}_2$$

$$= \varepsilon^0 \left(C_{1,0} + \frac{C_{2,0}}{r^m} \right) + \varepsilon^1 \left(C_{1,1} + \frac{C_{2,1}}{r^m} + \frac{C_{2,0}^2}{2r^{2m}} \right) + \varepsilon^2 \left(C_{1,2} + \frac{C_{2,2}}{r^m} + \frac{\chi}{2r^{2m}} + \frac{C_{2,0}^3}{2r^{3m}} \right) + O(\varepsilon^3).$$

The above solution is valid for the case with $m \neq 0$. The case with $m = 0$ which describes a homogeneous material with temperature-dependent material properties needs special attention. In this case, the zeroth-order solution reads

$$(3.30) \quad \bar{\vartheta}_0(r) = C_{1,0} + C_{2,0} \ln r,$$

where the integration constants $C_{1,0}$ and $C_{2,0}$ are given by

$$(3.31) \quad C_{1,0} = \frac{\mu_o \gamma_i - \mu_i \gamma_o}{\alpha_i \mu_o - \alpha_o \mu_i}, \quad C_{2,0} = \frac{\alpha_i \gamma_o - \alpha_o \gamma_i}{\alpha_i \mu_o - \alpha_o \mu_i},$$

in which

$$(3.32) \quad \mu_i = \alpha_i \ln R_i + \frac{\beta_i}{R_i}, \quad \mu_o = \alpha_o \ln R_o + \frac{\beta_o}{R_o}.$$

The first-order solution can also be obtained as

$$(3.33) \quad \bar{\vartheta}_1(r) = C_{1,1} + C_{2,1} \ln r + \frac{C_{2,0}^2}{2} \ln^2 r,$$

in which the integration constants $C_{1,1}$ and $C_{2,1}$ are obtained by applying the boundary conditions:

$$(3.34) \quad C_{1,1} = \frac{\mu_o \sigma_i - \mu_i \sigma_o}{\alpha_i \mu_o - \alpha_o \mu_i}, \quad C_{2,1} = \frac{\alpha_i \sigma_o - \alpha_o \sigma_i}{\alpha_i \mu_o - \alpha_o \mu_i},$$

in which

$$(3.35) \quad \begin{aligned} \sigma_i &= -C_{2,0}^2 \left(\frac{\alpha_i}{2} \ln^2 R_i + \beta_i \frac{\ln R_i}{R_i} \right), \\ \sigma_o &= -C_{2,0}^2 \left(\frac{\alpha_o}{2} \ln^2 R_o + \beta_o \frac{\ln R_o}{R_o} \right). \end{aligned}$$

Finally, the second-order solution is as follows:

$$(3.36) \quad \bar{\vartheta}_2(r) = C_{1,2} + C_{2,2} \ln r + \Lambda \ln^2 r + \frac{C_{2,0}^3}{2} \ln^3 r,$$

in which

$$(3.37) \quad \Lambda = \frac{C_{2,0}}{2} (C_{1,0} C_{2,0} + 2C_{2,1}).$$

Imposition of boundary conditions yields the following formulae for the integration constants $C_{1,2}$ and $C_{2,2}$:

$$(3.38) \quad C_{1,2} = \frac{\mu_o \tau_i - \mu_i \tau_o}{\alpha_i \mu_o - \alpha_o \mu_i}, \quad C_{2,2} = \frac{\alpha_i \tau_o - \alpha_o \tau_i}{\alpha_i \mu_o - \alpha_o \mu_i},$$

in which

$$(3.39) \quad \begin{aligned} \tau_i &= -\frac{2\beta_i \Lambda}{R_i} \ln R_i - \left(\alpha_i \Lambda + \frac{3\beta_i C_{2,0}^3}{2R_i} \right) \ln^2 R_i - \frac{\alpha_i C_{2,0}^3}{2} \ln^3 R_i, \\ \tau_o &= -\frac{2\beta_o \Lambda}{R_o} \ln R_o - \left(\alpha_o \Lambda + \frac{3\beta_o C_{2,0}^3}{2R_o} \right) \ln^2 R_o - \frac{\alpha_o C_{2,0}^3}{2} \ln^3 R_o. \end{aligned}$$

Now, the approximate temperature fields for $m = 0$ can be obtained using equations (3.4), (3.5) and (3.6).

The problem of steady one-dimensional conduction in an inhomogeneous hollow cylinder with temperature-dependent heat conductivity can be exactly solved as well. For this purpose, we start with the heat equation:

$$(3.40) \quad \frac{d}{dr} \left(r\lambda \frac{d\vartheta}{dr} \right) = \frac{d}{dr} \left(rf(r)g(\vartheta) \frac{d\vartheta}{dr} \right) = 0.$$

This results in the following implicit general solution:

$$(3.41) \quad \lambda_0\vartheta - \frac{1}{2}\lambda_1\vartheta^2 = \frac{C_1}{r^m} + C_2.$$

This is a quadratic equation for ϑ which can be solved to yield the temperature field ϑ . But, this approach has at least two problems. First, only first-kind boundary conditions can be imposed on this exact solution and the imposition of second- and third-kind boundary conditions is not possible. The second problem arises when a thermoelastic analysis is to be performed using the so-obtained temperature field. If this is the case, then the mathematical form of ϑ makes the thermoelastic analysis extremely difficult and in most cases a closed-form solution can not be obtained. However, the proposed perturbation solution does not exhibit these two problems and is therefore viable. Although the perturbation solution is valid when ε is very small, the approximate solution shows considerable improvement over the linear solution even when ε is not very small, as shown in Section 5.

4. Thermal stresses

Thermal stresses due to the obtained temperature field are considered here for the case of plane stress. The elasticity modulus E and the thermal expansion coefficient α_t are assumed to be temperature-independent and are only functions of the radial direction r whereas the Poisson's ratio ν is assumed to be constant. The static equilibrium equation for axisymmetric thermal stresses in a hollow cylinder reads

$$(4.1) \quad \frac{d\sigma_r}{dr} + \frac{\sigma_r - \sigma_t}{r} = 0,$$

where σ_r and σ_t are the radial and hoop stresses, respectively. In case of axisymmetric mechanical and thermal loading, the only non-zero displacement component is the radial one, denoted by u . The radial and tangential strains are related to u via

$$(4.2) \quad \epsilon_r = \frac{du}{dr}, \quad \epsilon_t = \frac{u}{r}.$$

The stress-strain relations are given by

$$(4.3) \quad \sigma_r = \frac{E(r)}{1-\nu^2} [\epsilon_r + \nu\epsilon_t - (1+\nu)\alpha_t(r)\vartheta_i],$$

$$(4.4) \quad \sigma_t = \frac{E(r)}{1-\nu^2} [\nu\epsilon_r + \epsilon_t - (1+\nu)\alpha_t(r)\vartheta_i],$$

in which $i = 0, 1, 2$. Substituting the kinematic equations (4.2) into constitutive equations (4.3) and (4.4) yields

$$(4.5) \quad \sigma_r = \frac{E(r)}{1-\nu^2} \left[\frac{du}{dr} + \nu \frac{u}{r} - (1+\nu)\alpha_t(r)\vartheta_i \right],$$

$$(4.6) \quad \sigma_t = \frac{E(r)}{1-\nu^2} \left[\nu \frac{du}{dr} + \frac{u}{r} - (1+\nu)\alpha_t(r)\vartheta_i \right].$$

Combining equations (4.1), (4.5) and (4.6) gives the following differential equation governing the displacement field u :

$$(4.7) \quad \frac{d^2u}{dr^2} + \left(\frac{1}{E} \frac{dE}{dr} + \frac{1}{r} \right) \frac{du}{dr} + \left(\frac{\nu}{Er} \frac{dE}{dr} - \frac{1}{r^2} \right) u = \frac{1+\nu}{E} \frac{d}{dr} (E\alpha_t\vartheta_i).$$

The material properties E and α_t are taken to be the following functions of r :

$$(4.8) \quad E(r) = E_0 \left(\frac{r}{R_o} \right)^p, \quad \alpha_t(r) = \alpha_{t0} \left(\frac{r}{R_o} \right)^q.$$

With this, the displacement equation (4.7) reads

$$(4.9) \quad r^2 \frac{d^2u}{dr^2} + (p+1)r \frac{du}{dr} + (\nu p - 1)u = \text{RHS}_i,$$

where RHS_i for $i = 0, 1, 2$ is given by

$$(4.10) \quad \text{RHS}_0 = \frac{\Gamma C_{1,0}}{r} + \frac{(\Gamma - m)C_{2,0}}{r^{m+1}},$$

$$(4.11) \quad \text{RHS}_1 = \frac{\Gamma A_1}{r} + \frac{(\Gamma - m)B_1}{r^{m+1}} + \frac{(\Gamma - 2m)C_1}{r^{2m+1}},$$

$$(4.12) \quad \text{RHS}_2 = \frac{\Gamma A_2}{r} + \frac{(\Gamma - m)B_2}{r^{m+1}} + \frac{(\Gamma - 2m)C_2}{r^{2m+1}} + \frac{(\Gamma - 3m)D_2}{r^{3m+1}},$$

in which $\Gamma = p + q - 1$.

The inhomogeneous ordinary differential equation (4.9) subjected to appropriate boundary conditions can be readily solved to yield the displacement field u . Once, u is known, stresses and strains can be easily calculated.

5. Numerical example

In this section, some selected results obtained from the proposed analytical solution are presented. As pointed out by equation (3.2), the actual values of material properties λ_0 and λ_1 are immaterial for the determination of the steady temperature field. Instead, the ratio λ_1/λ_0 which is denoted by ε the ratio influences the field. In this section, results of a temperature field at different levels of approximation obtained by setting $\alpha_i = 1$, $\alpha_o = 1$, $\beta_i = 0$, $\beta_o = 0$, $\gamma_i = 0$ and different values for γ_o are presented and compared with a numerical solution of the full nonlinear equation. The numerical solution is obtained by using a second-order central finite difference scheme. The simulation is conducted on a very fine computational mesh so that the solution can be considered as “exact” within the round-off error margin of the computer. The code has been written in Fortran and the simulation has been conducted in the double precision mode of the compiler.

Figure 1 shows the temperature profiles for $\vartheta_i = 0^\circ\text{C}$, $\vartheta_o = 1000^\circ\text{C}$, $\varepsilon = 0.001$ and $m = 0$ obtained by different orders of approximation. The solution of full nonlinear governing equations obtained by an accurate numerical solution based on the finite difference method is also plotted for comparison. The convergence of perturbation series from the zeroth-order solution (i.e., the linear problem) towards the “exact” solution by increasing the order of approximation is demonstrated in this figure. However, even the second-order approximation does not fully match the numerical solution. If the value of ε decreases then the accuracy of the solution is significantly improved.

It is worthwhile to note that the “exact” temperature profile is concave up. However, it is observed at the first glance that the zeroth-order solution, i.e., the linear solution, is concave down. This means that the linear description not only fails to quantitatively predict the full solution, but it also fails in the qualitative prediction of the physics. Moreover, the neat feature of higher-order approximations is observed as the first- and second-order solutions show concave-up temperature profiles. Though, the concave-up feature of the first-order solution is modest. This observation confirms that the proposed asymptotic solution procedure is neat in predicting the concavity of the temperature profiles. It shall be mentioned that the protuberance which occurred in the “exact” temperature profile in the vicinity of the outer surface is not reproduced by any of approximate solutions up to the second order. This discrepancy can be alleviated by going to even higher orders, cf. [15]. However, at smaller values of ε , as discussed below, the protuberance disappears and the approximation is just fine.

To demonstrate the effect of ε on the convergence of the asymptotic series, the temperature fields obtained by the aforementioned set of parameters but with $\varepsilon = 0.0005$ and $\varepsilon = 0.0001$ are respectively depicted in Figs. 2 and 3. It is

instrumental to note that these values of ε are typical for engineering materials, e.g. for steel we have $\varepsilon = 0.000584$. We conclude that the greater the value of ε , the more terms in the asymptotic series are required to retain a given accuracy.

In order to show the effect of temperature difference between the inner and outer surfaces of the cylinder, temperature profiles for $\gamma_o = 500^\circ\text{C}$ and

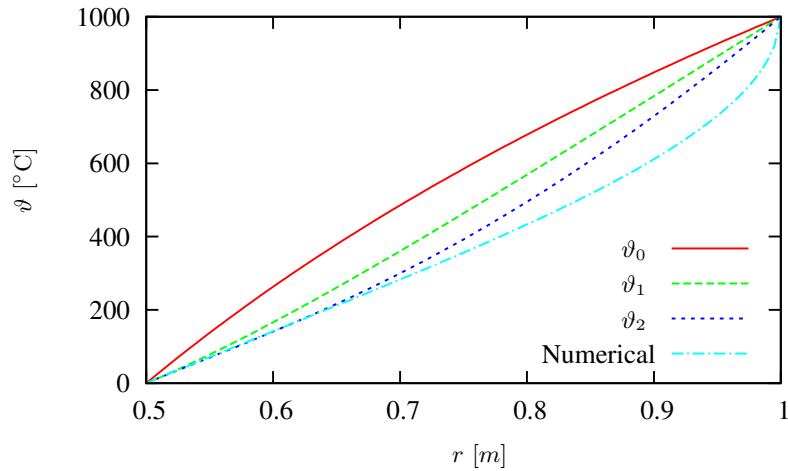


FIG. 1. Temperature profiles for $\gamma_o = 1000^\circ\text{C}$, $\varepsilon = 0.001$ and $m = 0$ obtained by different orders of approximation and compared with a numerical solution of the full nonlinear equation.

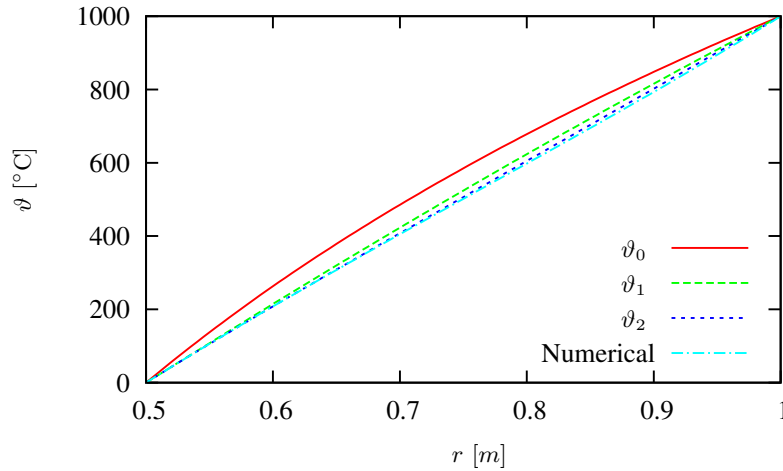


FIG. 2. Temperature profiles for $\gamma_o = 1000^\circ\text{C}$, $\varepsilon = 0.0005$ and $m = 0$ obtained by different orders of approximation and compared with a numerical solution of the full nonlinear equation.

$\gamma_o = 100^\circ\text{C}$ with $\varepsilon = 0.001$ and $m = 0$ are depicted in Figs. 4 and 5, respectively. In Figs. 4, we see that ϑ_2 almost coincides with the “exact” solution while ϑ_1 is a little bit off. By decreasing γ_o even more, in Fig. 5 both ϑ_1 and ϑ_2 almost coincide with the “exact” solution. It means that the higher the temperature difference, the more terms in the perturbation series are required in order to get an accurate solution.

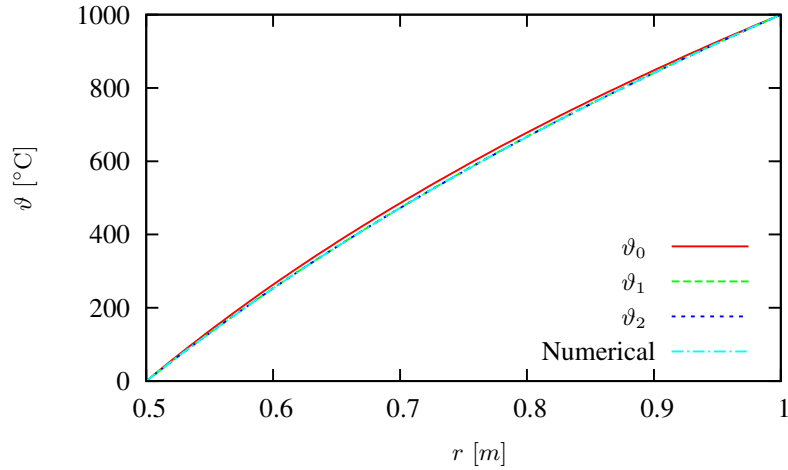


FIG. 3. Temperature profiles for $\gamma_o = 1000^\circ\text{C}$, $\varepsilon = 0.0001$ and $m = 0$ obtained by different orders of approximation and compared with a numerical solution of the full nonlinear equation.

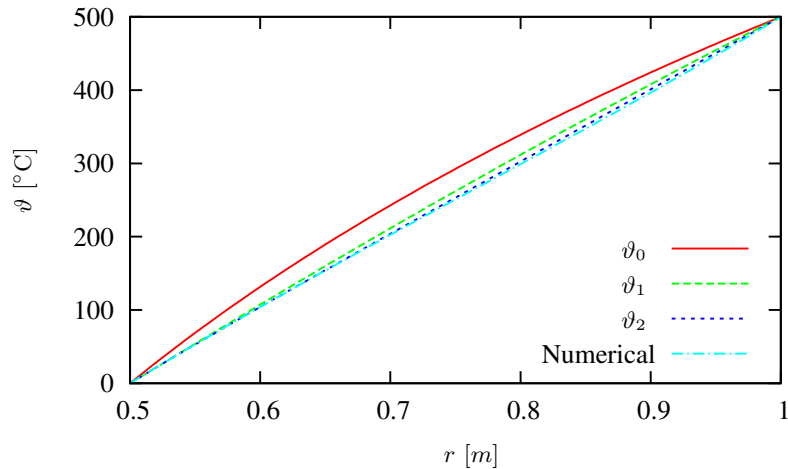


FIG. 4. Temperature profiles for $\gamma_o = 500^\circ\text{C}$, $\varepsilon = 0.001$ and $m = 0$ obtained by different orders of approximation.

The ϑ_2 profiles presented in Fig. 6 are obtained by setting $\gamma_o = 1000^\circ\text{C}$ and $\varepsilon = 0.0005$ for various values of m . Figure 6 shows how the value of m affects the temperature profile. Larger values of m lead to higher temperature levels and vice versa. Also, the curvature of temperature curves changes with the values of m . This means that for large positive values of m , the temperature gradient near the inner surface is sharp and this sharp gradient weakens by

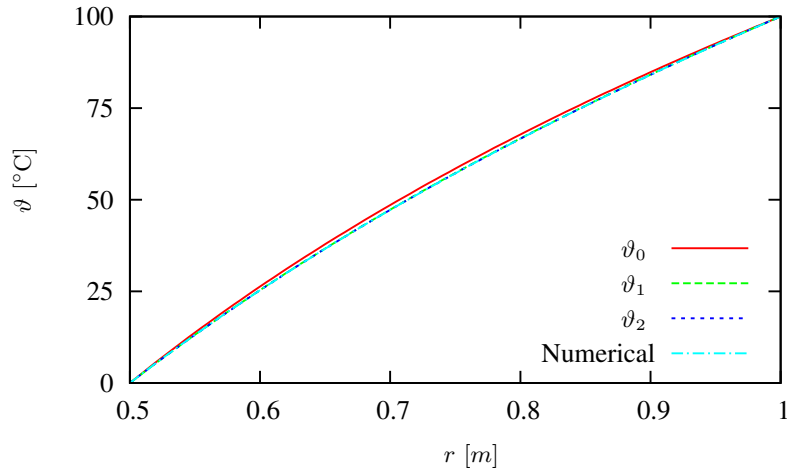


FIG. 5. Temperature profiles for $\gamma_o = 100^\circ\text{C}$, $\varepsilon = 0.001$ and $m = 0$ obtained by different orders of approximation.

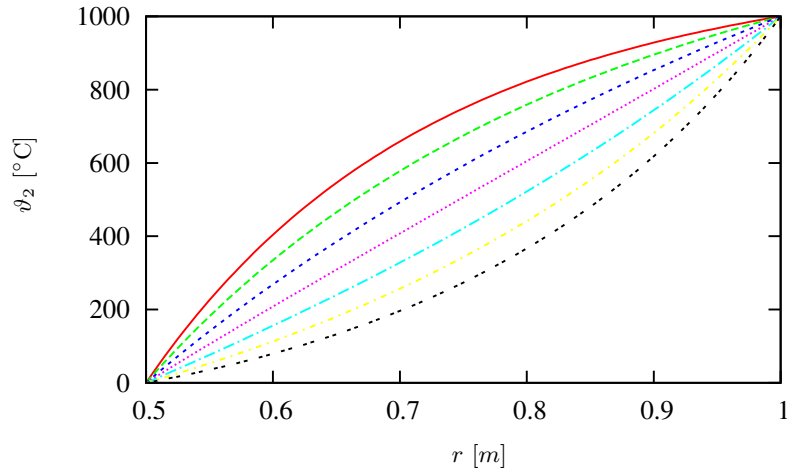


FIG. 6. Temperature profiles ϑ_2 for $\gamma_o = 1000^\circ\text{C}$, $\varepsilon = 0.0005$ and various values m . From top to the bottom, the values of m are 3, 2, 1, 0, -1, -2 and -3.

approaching the outer surface. However, for negative values of m , the behavior is converse. This trend can be explained as follows. For positive m , the heat conductivity assumes its minimum value at the inner surface and it increases by approaching the outer surface. Moreover, the radial heat flux is constant in this one-dimensional problem. Thus, by increasing λ in the radial direction, the temperature gradient $\partial\vartheta/\partial r$ has to decrease in order to retain a constant heat flux. A converse statement holds for the negative values of m .

6. Conclusions

In this paper, an approximate analytical solution for the temperature field in a hollow cylinder made of FGM with temperature-dependent material properties is presented. After introducing the governing equations and the boundary conditions of the problem, the heat conduction problem is analytically solved using perturbation technique. This leads to an approximate solution, but the order of accuracy can be increased in a systematic manner. The convergence of the hierarchical asymptotic solutions is examined by comparison to a numerical solution of the full nonlinear problem. Finally, a numerical example is worked out and some of the temperature profiles are presented and discussed.

References

1. M. AZADI, M. AZADI, *Nonlinear transient heat transfer and thermoelastic analysis of thick-walled FGM cylinder with temperature-dependent material properties using Hermitian transfinite element*, J. Mech. Sci. Tech., **23** (2009), 2635–2644.
2. Y. OBATO, N. NODA, *Thermal stress in hollow circular cylinder and a hollow sphere of a functionally graded material*, J. Thermal Stresses, **14** (1994), 471–487.
3. Y. OOTAO, T. AKAI, Y. TANIGAWA, *Three-dimensional transient thermal stress analysis of a nonhomogeneous hollow circular cylinder due to a moving heat source in the axial direction*, J. Thermal Stresses, **18** (1995), 497–512.
4. M.P. LUTZ, R.W. ZIMMERMAN, *Thermal stresses and effective thermal expansion coefficient of a functionally graded sphere*, J. Thermal Stresses, **19** (1996), 39–54.
5. R.W. ZIMMERMAN, M.P. LUTZ, *Thermal stress and effective thermal expansion in a uniformly heated functionally graded cylinder*, J. Thermal Stresses, **22** (1999), 177–188.
6. Y. TANIGAWA, H. MORISHITA, S. OGAKI, *Derivation of system of fundamental equations for a three-dimensional thermoelastic field with nonhomogeneous material properties and its application to a semi-infinite body*, J. Thermal Stresses, **22** (1999), 689–711.
7. M. JABBARI, S. SOHRABPOUR, M.R. ESLAMI, *Mechanical and thermal stresses in functionally graded hollow cylinder due to radially symmetric loads*, Int. J. Pressure Vessels Piping, **79** (2002), 493–497.

8. M. JABBARI, S. SOHRABPOUR, M.R. ESLAMI, *General solution for mechanical and thermal stresses in a functionally graded hollow cylinder due to nonaxisymmetric steady-state loads*, ASME J. Appl. Mech., **70** (2003), 111–118.
9. K.M. LIEW, S. KITIPORNCHAI, X.Z. ZHANG, C.W. LIM, *Analysis of the thermal stress behaviour of functionally graded hollow circular cylinders*, Int. J. Solids Structures, **40** (2003), 2355–2380.
10. L.H. YOU, J.J. ZHANG, X.Y. YOU, *Elastic analysis of internally pressurized thick-walled spherical pressure vessel of functionally graded materials*, Int. J. Pressure Vessels Piping, **82** (2005), 347–354.
11. J. ZHAO, X. AI, Y.Z. LI, *Transient temperature fields in functionally graded materials with different shapes under convective boundary conditions*, Heat Mass Transfer, **43** (2007), 1227–1232.
12. Y.Z. CHEN, X.Y. LIN, *Elastic analysis for thick cylinders and spherical pressure vessels made of functionally graded materials*, Comput. Mater. Sci., **44** (2008), 581–587.
13. M. ASGARI, M. AKHLAGHI, *Transient heat conduction in two-dimensional functionally graded hollow cylinder with finite length*, Heat Mass Transfer, **45** (2009), 1383–1392.
14. X.L. PENG, X.F. LI, *Thermo-elastic analysis of a cylindrical vessel of functionally graded materials*, Int. J. Pressure Vessels Piping, **87** (2010), 203–210.
15. A. MOOSAIE, *Steady symmetrical temperature field in a hollow spherical particle with temperature-dependent thermal conductivity*, Arch. Mech., **64** (2012), 405–422.

Received October 13, 2014; revised version March 22, 2015.
